Electron-Ion Path Integral Monte Carlo

Riccardo Fantoni*
Università di Trieste, Dipartimento di Fisica, strada Costiera 11, 34151 Grignano (Trieste), Italy
(Dated: May 1, 2026)

We performed numerical (restricted) path integral Monte Carlo experiments on metallic Hydrogen from first principles. We study a quantum two component plasma where one component is made of pointwise particles of negative unitary charge and the other is made of charged hard spheres of positive unitary charge. We study both the additive mixture and a nonadditive mixture where we only keep a hard core between unlike species. We specialize to the case of the electron-proton plasma with a 1:1 ratios between the molar fraction of the two species. We measured thermodynamic and structural properties of the plasma. From an analysis of the structure we see a transition from a metallic Hydrogen phase, to a molecular Hydrogen phase as the temperature is lowered. As expected at high density the correlations are diminished.

Keywords: Path Integral; Monte Carlo; Quantum Mixture; Bosons; Fermions; Two Component Plasma; Thermodynamics; Structure; Superfluidity; Sign Problem; Metallic Hydrogen; Molecular Hydrogen; Hydrogen Atom; Hydrogen Molecule

CONTENTS

I. INTRODUCTION

Hydrogen is the simplest element in the Universe. It has a nucleus made of only one proton, the ion, and an orbiting electron. An interesting question is whether the laws of quantum statistical physics and of Coulomb are able to reproduce the *formation of the Hydrogen atoms* given a plasma made of an equal number of electrons and protons, a Two Component Plasma (TCP). This problem has been widely studied in literature starting from the pioneering exact analytic study of the non quantum TCP in one dimension of Edwards and Lenard [1, 2] to reach the realistic first principles ground state Monte Carlo calculations of Ref. [3] and non zero temperature Path Integral Monte Carlo (PIMC) calculations of Refs. [4, 5] or the coupled electron-ion Monte Carlo [6] where the ground state properties of the electrons component are used to perform a PIMC calculation on the protons component only.

There are many non quantum simulations of the TCP studying the clustering and phase transition properties [7]. Here we want to study the quantum version specializing to the electron-proton binary mixture with a 1:1 ratios between the particle numbers of the two species. This will allow us to investigate the Hydrogen atom formation problem.

We then start from a completely ionized TCP with a number $N_e = N/2$ of polarized electrons equal to the number $N_p = N/2$ of polarized protons in a volume Ω and in thermal equilibrium at an inverse temperature $\beta = 1/k_B T$ with k_B Boltzmann constant and T the absolute temperature. We use a PIMC calculation [8] with a number $M = \beta/\tau$

* riccardo.fantoni@scuola.istruzione.it

of timeslices of length τ which discretize the imaginary time interval $[0, \beta[$ to determine the thermodynamic and structural properties of the plasma. In particular the structural clustering that we observe proves the ability of the quantum statistical physics theory to predict the atom formation from first principles when one introduces just Coulomb pair interactions. [1]

Since the proton is about 2000 times more heavy than the electron we expect the protons species paths to be much more contracted than the ones of the electrons species. But, as we will see, this occurrence does not pose any serious limitation to what can be simulated but only an increase of the computer time needed to measure the properties of the protons component.

We know that both the electron and the proton are spin 1/2 identical particles and as such they each obey to the Fermi-Dirac statistics. But as we will see there is just a slight difference between treating both species as fermions or as bosons. This is essentially due to the property of bosons to 'like' themselves and of the fermions to 'dislike' themselves. Of course while bosons simulations are exact, fermions simulations are affected by the so called 'fermions sign problem' [9] which can be overcome only by approximate methods like the Restricted PIMC (RPIMC) [10]. The approximate RPIMC for fermions is much more slow than the exact PIMC for bosons since it requires the calculation of M determinants of dimension $N/2$ at each Metropolis attempted move [11]. So that only small N systems can be studied.

Due to the divergence of the Coulomb potential at contact like $1/r$ it is necessary to introduce a hard core of diameter σ for the nuclei, the protons, while we will consider the electrons as dimensionless and pointwise. This is needed in order to obtain a stable many body system that does not collapse. As we will see, for a given temperature T, the minimum hard core diameter preventing the collapse will be dependent from temperature, $\sigma = \sigma_{\min}(T)$.

We will investigate both the additive mixture when the pointwise electrons cannot get closer than $\sigma/2$ to the protons and two protons cannot get closer than σ among themselves and the nonadditive mixture [7, 12] when both the electrons and the protons are pointwise among themselves but the electron still cannot get closer than $\sigma/2$ to a proton. This analysis will show how introducing a hard core between the protons is largely unnecessary. In fact the nonadditive scenario is sufficient to "dress" the protons with the electronic cloud which is able to keep two protons roughly a distance σ apart spontaneously.

II. PIMC OF A TCP AND RPIMC OF METALLIC HYDROGEN

Let us consider an additive mixture of polarized electrons, e, and polarized protons, p. [2] First of all let us define our reduced units. We measure masses in units of the electron mass m_e so that the reduced mass of the electron will be $\mu_e = m_e/m_e = 1$ and the reduced mass of the proton $\mu_p = m_p/m_e \approx 1836.15$. The characteristic kinetic energy is

$$\mathscr{K} = \frac{\hbar^2}{2m_e\ell^2}, \tag{2.1}$$

with ℓ a length. The characteristic Coulomb energy is

$$\mathscr{V} = \frac{e^2}{\ell} = \frac{2\mathscr{K}\ell}{\mathscr{L}}, \tag{2.2}$$

with e the electron charge magnitude and

$$\mathscr{L} \approx 5.29177 \times 10^{-9}\text{cm} \tag{2.3}$$

the Bohr radius $a_B = \hbar^2/m_e e^2$. Then, if we denote with $n = N/\Omega$ the reduced number density this will correspond to a real number density of $n\mathscr{L}^{-3}$ in cm^{-3}. For example for metallic Hydrogen we have a mass density $\approx 1\text{g/cm}^3$ which corresponds to a reduced number density of $n \approx \mathscr{L}^3 2/m_p \approx 0.177189$.

We may then take as characteristic temperature

$$\mathscr{T} = \frac{2\mathscr{K}\ell^2}{\mathscr{L}^2 k_B} \approx 315775\text{K}. \tag{2.4}$$

So that for metallic Hydrogen in planetary interiors, like for Jupiter for example, an absolute temperature of $\approx 10^4$K will correspond to a reduced temperature of $T \approx 10^4/\mathscr{T} \approx 0.0316681$.

---

[1] It would be interesting to see if, for more complicated atoms, the introduction of nuclear forces would still make it possible to predict the atom formation.

[2] Here we choose polarized particles for simplicity but in the most general setting one would require a four component mixture with spin up and down electrons and spin up and down protons.

The diameter of the nucleus of the Hydrogen atom is of the order of a fermi, i.e. $\approx 1\text{fm} = 1 \times 10^{-13}\text{cm}$ which in reduced units is $\sigma_{\text{H}} \approx 1.88973 \times 10^{-5}$. On the other hand we will consider the electrons as pointwise. The electrons will collapse onto the protons as soon as their kinetic energy is less than the Coulomb attraction at contact. In reduced units this balance can be rudely estimated by $T \lesssim 1/\sigma$. Therefore choosing the Hydrogen nucleus size, σ_{H}, as the protons hard core, σ, requires a temperature larger than 10^{10}K to grant ionization of the mixture against collapse. Moreover, upon collapse, the Coulomb energy at contact between a proton and the collapsed electron will be $1/\sigma_{\text{H}}$ in units of e^2/a_B, i.e. of two Rydbergs. If we have collapse and we use Bose-Einstein statistics between the like particles the whole system of (neutral) atoms may further collapse to a point, a giant cluster of atoms.

In order to estimate the cutoff reduced distance $r_0 = \sigma/2$ in the Coulomb attractive potential between an electron and a proton we note that the path averaging in the Feynman-Kac formula smooths the potential. The smoothing makes the action finite at the origin instead of having a $1/r$ singularity [8, 13]. The cusp condition for the pair Coulomb density matrix requires a behavior as $\sim r/(1/\mu_1 + 1/\mu_2) \sim r\mu_2$ as the electron approaches a proton at a small distance r. Setting this equal to their primitive inter-action τ/r we find

$$r_0 \sim \sqrt{\frac{\tau}{\mu_2}} \sim 0.023\sqrt{\tau}, \tag{2.5}$$

in reduced units.

Summarizing, in our reduced units we will measure lengths in units of a Bohr radius a_B and energies in units of two Rydbergs e^2/a_B, i.e. of a Hartree. The Hamiltonian and the density matrix in reduced units will then read

$$H = K + V = -\sum_{\alpha=1}^{N} \frac{1}{2\mu_{i_\alpha}} \nabla_\alpha^2 + \sum_{\alpha<\beta=1}^{N} \phi_{i_\alpha i_\beta}(r_{\alpha\beta}), \tag{2.6}$$

$$\rho = e^{-H/T}. \tag{2.7}$$

where we indicate with a Greek index the particle label and with a Roman index the species label so that for example i_α is the species label of particle α, either 1 for the electrons or 2 for the protons, $\boldsymbol{r}_\alpha$ is the position vector of particle α, and $r_{\alpha\beta} = |\boldsymbol{r}_{\alpha\beta}| = |\boldsymbol{r}_\alpha - \boldsymbol{r}_\beta|$ is the distance between particles α and β. Distances are measured in units of $\mathscr{L}$. The reduced masses are then $\mu_1 = \mu_e$ and $\mu_2 = \mu_p$. The partial pair potential ϕ_{ij} is the usual Coulomb potential given by

$$\phi_{ij}(r) = \begin{cases} \epsilon_{ij}/r & r > \Sigma_{ij} \\ \infty & \text{else} \end{cases}, \tag{2.8}$$

where in the Two-Component-Plasma (TCP) we choose

$$\boldsymbol{\epsilon} = \begin{pmatrix} 1 & -1 \\ -1 & 1 \end{pmatrix}, \tag{2.9}$$

$$\boldsymbol{\Sigma} = \begin{pmatrix} 0 & \sigma/2 \\ \sigma/2 & \sigma \end{pmatrix}. \tag{2.10}$$

Note that at a given T if we choose σ too small the whole system collapses with all the negative light particles falling onto the heavy positive particles.

We will indicate with N_i the number of particles of species $i = 1, 2$ and $N = \sum_i N_i$ the total number of particles with $x_i = N_i/N$ the molar fraction for species i such that $\sum_i x_i = 1$. The reduced partial number densities $n_i = n x_i$ [3] with $n = N/\Omega$ and, in a cubic box, $\Omega = L^3$, with L the reduced length of the box side.

Note that one could introduce for each species some length scales

$$\mathscr{W}_i = n_i^{-1/3}, \quad i = 1, 2 \tag{2.11}$$

and rescale each reduced coordinate as $\tilde{\boldsymbol{r}}_\alpha = \boldsymbol{r}_\alpha/\mathscr{W}_{i_\alpha}$. Then the rescaled kinetic energy of species i, $\tilde{K}_i = \mathscr{W}_i^2 K_i$ and the rescaled potential energy of species i, $\tilde{V}_i = \mathscr{W}_i V_i$. We then see that as n_i increases V_i is penalized respect to K_i and that component tends to behave more like a "free" gas with less correlations. This is confirmed by our numerical experiments.

The box can be made periodic so that it permeates the whole infinite three dimensional space in order to mimic the thermodynamic limit. This will produce finite size errors that can be reduced by increasing the box size L. Of

---

[3] Sometimes it can be useful to work in terms of the Wigner-Seitz radius r_s for the electron component, i.e. $r_s = (4\pi n_1/3)^{-1/3}$ the reduced mean inter-electron distance.

course in order to study a given thermodynamic state of the system this requires increasing L at constant density n which means increasing N. This will make the computer experiment more demanding from the numerical calculation cost point of view.

Moreover, in periodic boundary conditions the potential energy V for the particles within the central box should include also the pair interactions with all their images in the periodic boxes. Since the Coulomb potential $1/r$ is long range these contributions cannot generally be neglected and specific techniques should be used [14] to treat them, the most common of which is the Ewald summation. In this preliminary work we will simply neglect interactions with periodic images since we will not carry out a careful finite size error analysis.

We performed some computer experiments as described in Table I. During the simulations we measured some thermodynamic quantities as the total kinetic and potential energy of the TCP and the superfluid fractions for each species. These were measured using the thermodynamic estimators described in Ref. [8]. And we also calculated the partial and total radial distribution functions. Given an observable $\mathscr{O}$ we can measure it during the simulation through the following PIMC operation [8]

$$\langle \mathscr{O} \rangle = \mathrm{tr}(\rho \mathscr{O})/Z, \tag{2.12}$$

$$Z = \mathrm{tr}(\rho), \tag{2.13}$$

where ρ is the primitive approximation [8] for the density matrix of Eq. (2.7), $\mathrm{tr}(\ldots)$ is the trace operation, and Z is the canonical partition function. Therefore we impose both spatial and imaginary time periodic boundary conditions for the many body path of both species $R(t) = (\boldsymbol{r}_1(t), \boldsymbol{r}_2(t), \ldots, \boldsymbol{r}_N(t))$ so that for any function f we require $f(R + LU) = f(R)$ with $U = (1, 1, \ldots, 1)$ a $3N$ vector and $R(t + \beta) = R(t)$ with $\beta = 1/T$ the reduced inverse temperature. Our algorithm is discussed in the Appendix A

TABLE I. Cases treated in our simulations for the additive TCP with a pair Coulomb potential as in Eq. (2.8) with (2.9) and (2.10) (cases C,D,E,F,G correspond to the electron-proton plasma). The reduced masses of the two species are $\mu_1 = 1$ and μ_2, the molar fractions $x_1 = 1 - x_2$ and x_2, σ the hard core of species 2, the total number of particles N, the reduced density $n = N/\Omega$, the reduced inverse temperature $\beta = 1/T$, $e_K = \langle K \rangle / N$ the total kinetic energy per particle, $e_V = \langle V \rangle / N$ the total potential energy per particle, $f_s(i)$ the superfluid fraction for species i. These three thermodynamic quantities are measured from the thermodynamic estimators discussed in Ref. [8]. The other quantities were introduced in the main text. In the statistics column "b" stands for bosons, "f" for fermions. The simulation lasted more than 10^8 Monte Carlo steps where one step is made of a displace move of all the beads of a single particle path and a bridge move. The simulations for fermions lasted about one week of computer time.

case	statistics	β	M	n	N	x_2	μ_2	σ	Ne_K	$-Ne_V$	$f_s(1)$	$f_s(2)$
A	b (PIMC)	10	20	0.1	20	0.5	1000	0.4	5.26(2)	11.95(4)	0.520(5)	0.0477(2)
B	f (RPIMC)	10	20	0.1	20	0.5	1000	0.4	5.32(1)	12.20(2)	0.492(3)	0.0475(1)
C	b (PIMC)	10	20	0.08	20	0.5	1836.15	0.4	5.54(2)	12.81(4)	0.370(6)	0.0477(6)
D	f (RPIMC)	10	20	0.08	20	0.5	1836.15	0.4	5.02(1)	11.50(3)	0.501(4)	0.0475(1)
E	b (PIMC)	10	20	0.18	20	0.5	1836.15	0.4	5.86(2)	13.38(3)	0.557(5)	0.0478(2)
F	f (RPIMC)	10	20	0.18	20	0.5	1836.15	0.4	5.71(1)	13.08(1)	0.584(2)	0.0476(2)
G	b (PIMC)	200	20	0.16	20	0.5	1836.15	1	1.709(1)	23.56(2)	0.093(4)	0.0469(4)
H	f (RPIMC)	200	20	0.16	20	0.5	1836.15	1	1.708(1)	24.25(1)	0.072(2)	0.0475(3)

In Fig. 1 we show snapshots taken during the simulations of cases A and B of Table I. We see how the light and fast species is in a quantum regime with extended paths while the heavy and slow species is in a classical regime with contracted paths. In these cases $\tau = \beta/M = 0.5$ which is small. Fig. 2 shows the snapshots for the electron-proton plasma at low temperature of cases G and H of Table I. We see how in these cases also the protons are in a quantum regime with extended paths. We also see the formation of H atoms and of H_2 molecules. Note that in these cases $\tau\beta/M = 10$ which is rather big. We did not perform a careful study of the imaginary time discretization error since we are here only interested in the phenomenological and qualitative properties of the simulations. We leave to further works the extrapolation to the continuum $\tau \to 0$ limit necessary to extract quantitative results.

The partial pair correlation functions or partial Radial Distributions Functions (RDF), $g_{ij}(r)$, are a sensitive indicator of quantum and correlation effects and reflect the structural properties of the TCP. The like $i = j$ RDF is proportional to the probability that sitting on a particle of species i one has to find another particle of the same species within the radial interval $[r, r + dr]$, whereas the unlike RDF $i \neq j$ give the structure of species i as seen from

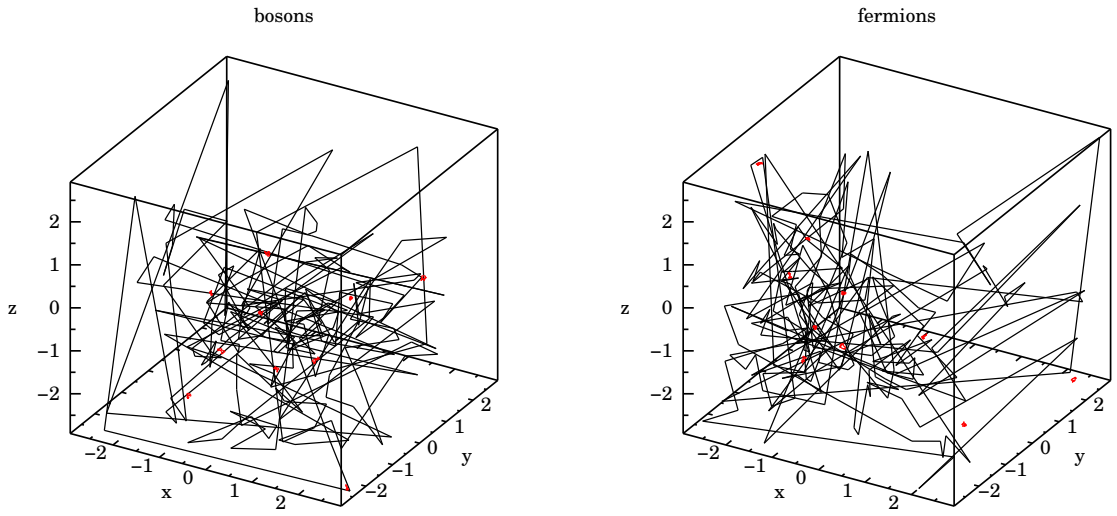

FIG. 1. Snapshots of the simulation of a binary mixture with $N = 20, x_1 = 1/2, \mu_1 = 1, \mu_2 = 1000, \sigma = 0.4$. The mixture is in a thermodynamic state with a reduced temperature $T = T'/\mathscr{T} = 0.1$ with T' measured in degrees Kelvin and a reduced number density $n = n'\mathscr{L}^3 = 0.1$ with n' measured in cm^{-3}. In the path integral we chose $M = 20$ and used either Bose-Einstein (left panel, case A in Table I) or Fermi-Dirac (right panel, case B in Table I) statistics among like particles. Red paths are for the heavy slow species and black paths are for the light fast species.

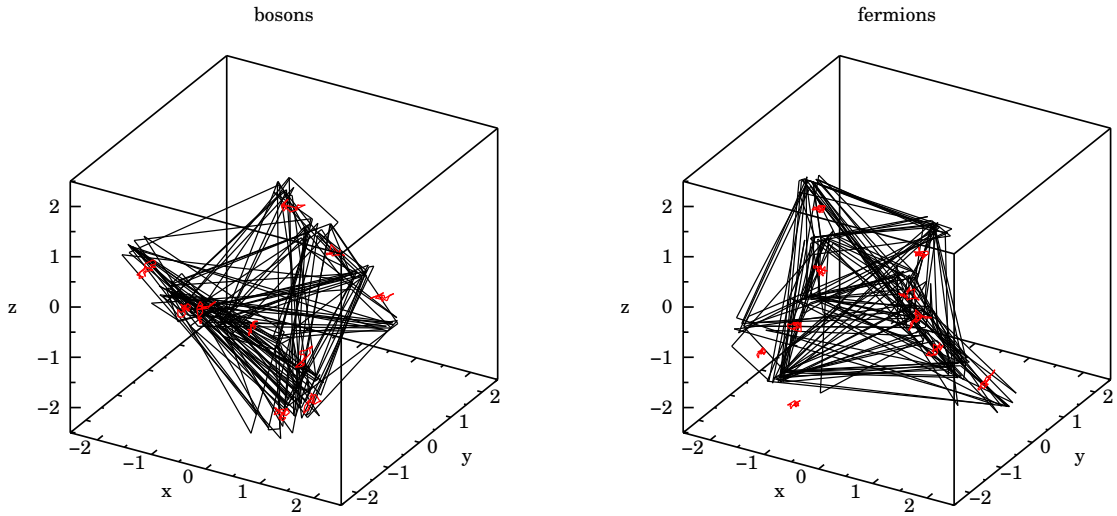

FIG. 2. Snapshots of the simulation of a binary mixture with $N = 20, x_1 = 1/2, \mu_1 = 1, \mu_2 = 1836.15, \sigma = 1$. The mixture is in a thermodynamic state with a reduced temperature $T = T'/\mathscr{T} = 0.005$ with T' measured in degrees Kelvin and a reduced number density $n = n'\mathscr{L}^3 = 0.16$ with n' measured in cm^{-3}. In the path integral we chose $M = 20$ and used either Bose-Einstein (left panel, case G in Table I) or Fermi-Dirac (right panel, case H in Table I) statistics among like particles. Red paths are for the heavy slow protons and black paths are for the light fast electrons.

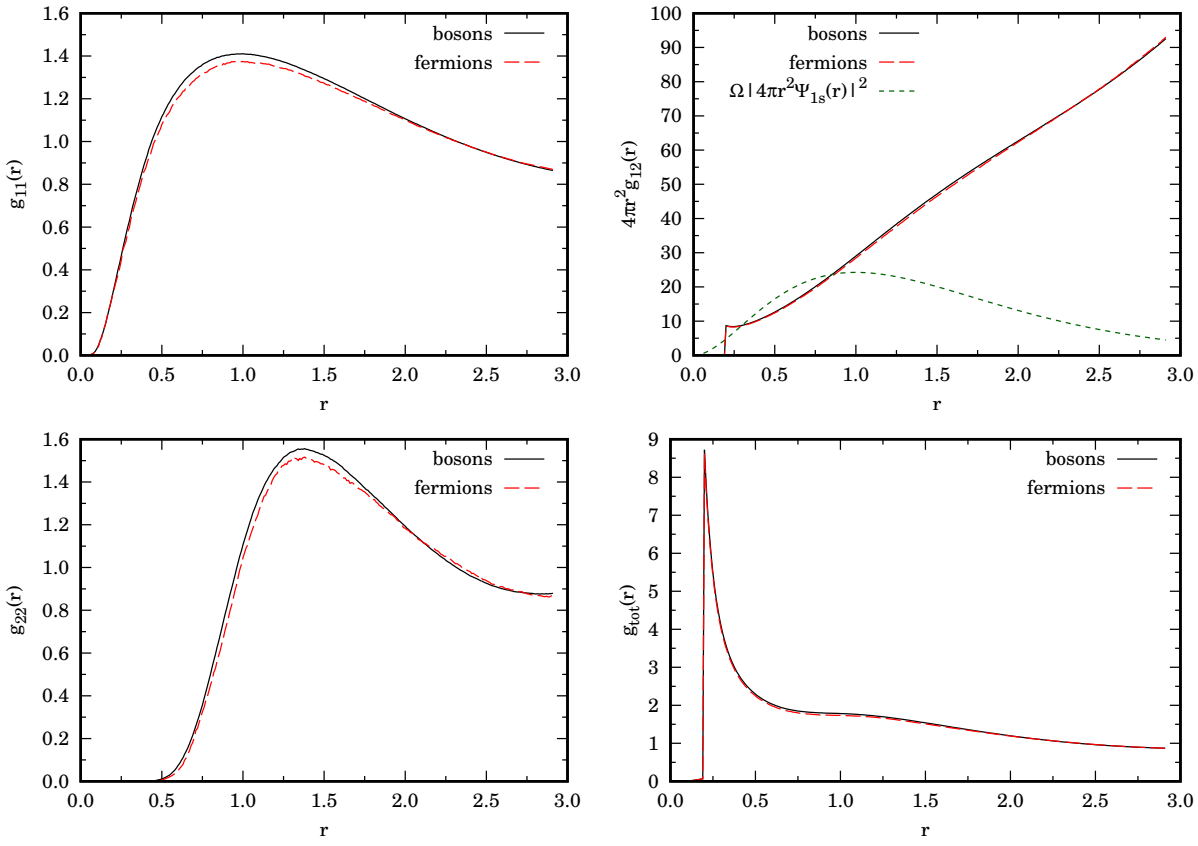

FIG. 3. The partial, g_{ij}, and total, g_{tot}, radial distribution functions for a binary mixture with $N = 20, x_1 = 1/2, \mu_1 = 1, \mu_2 = 1000, \sigma = 0.4$. In the panel for the unlike radial distribution function we also show the ground state probability distribution of the Hydrogen atom for comparison. The mixture is in a thermodynamic state with a reduced temperature $T = T'/\mathscr{T} = 0.1$ with T' measured in degrees Kelvin and a reduced number density $n = n'\mathscr{L}^3 = 0.1$ with n' measured in cm^{-3}. In the path integral we chose $M = 20$ and used either Bose-Einstein (case A in Table I) or Fermi-Dirac (case B in Table I) statistics among like particles. In the figures $r = r'/\mathscr{L}$ where r' is measured in centimeters.

the other species. The total RDF is defined as $g_{\mathrm{tot}} = x_1^2 g_{11} + 2x_1x_2g_{12} + x_2^2 g_{22}$. From Figs. 3,4,5, and 6 we see the formation of clusters made of an heavy positive particle (of species 2) surrounded by a cloud of light negative particles (of species 1). In the panel for the unlike RDF we compare with the electronic probability density corresponding to the isolated atom ground state $|\Psi_{1s}|^2$ which has a characteristic radial length equal to a Bohr radius a_B. In Fig. 3 we show results for cases A and B of Table I and we see that the species 1 develops a peak in g_{11} at $\sim a_B$ while the species 2 at $\sim 1.3a_B$ in g_{22}. In Fig. 4 we show results for cases C and D of Table I, in Fig. 4 we show results for cases E and F, and In Fig. 4 we show results for cases G and H. All these cases correspond to a realistic electron-proton plasma. We also see how changing the statistics between (identical) particles of the same species from Bose-Einstein to Fermi-Dirac makes them dislike themselves more as expected from the Pauli exclusion principle. Comparing Figs. 4 and 5 we see how the difference between the two statistics increases at higher densities for a given low temperature, as expected. Comparing the reduced de Broglie thermal wavelength $\Lambda_i = \sqrt{1/T\mu_i}$ with the interparticle spacing $n_i^{-1/3}$ we may define a reduced degeneracy temperature $T_i^D = n_i^{2/3}/\mu_i$ for each species. For temperatures higher than the degeneracy temperature, quantum statistics, either bosonic or fermionic, are not very important. Note that the difference between the two statistics for the heavy and slow protons component is driven by the light and fast electrons component which "dress" the protons.

From Fig. 5 we see how the oscillations in the proton-proton RDF, g_{22}, lower their radial length scale as density is increased, with a first peak around $\sim 1.3a_B$. Moreover the first peak in the like RDFs gets damped in agreement with our expectation to observe less correlations in this case. The magnitudes of the total kinetic and potential energies and of the superfluid fraction of the electron component all increase as only the number density of the electron-proton plasma is increased. As expected the superfluid fraction of the protons component is almost zero since the protons behave nearly classically without exchanges. So that the winding number for their paths is almost zero.

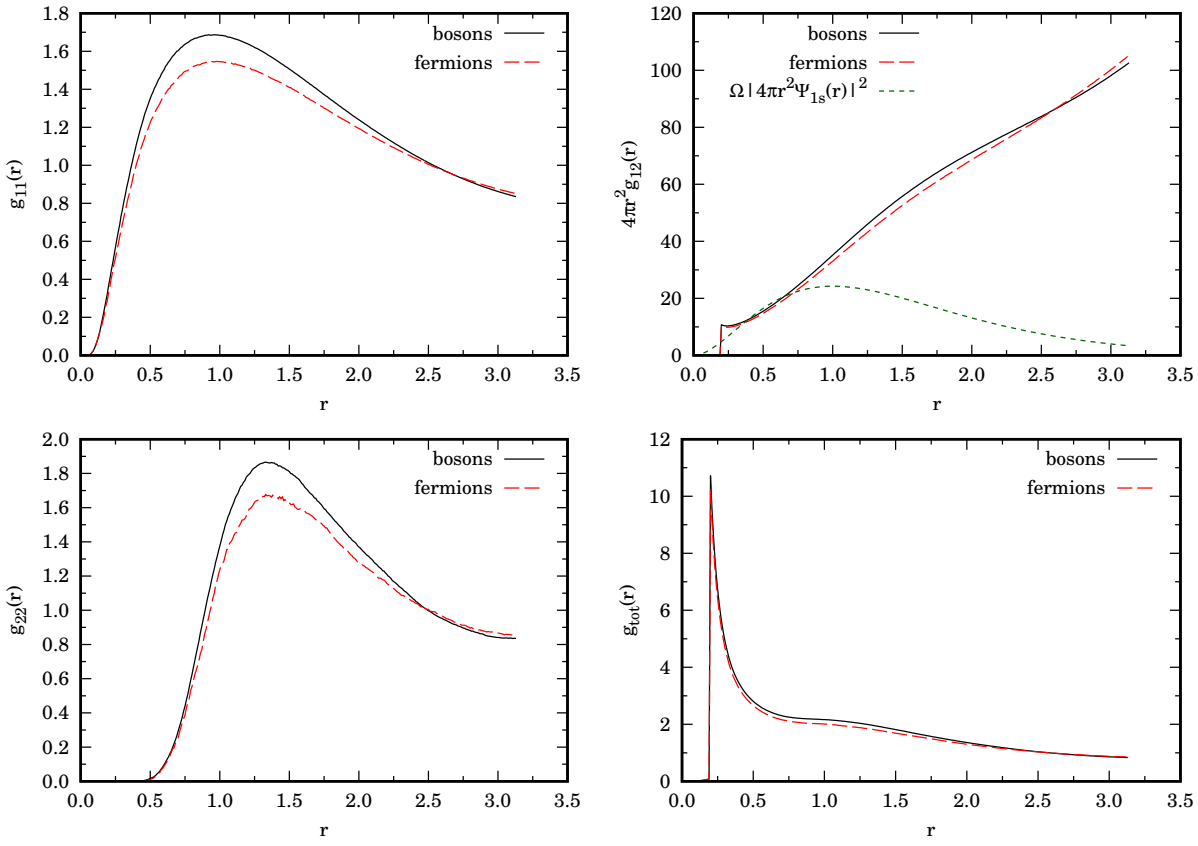

FIG. 4. The partial, g_{ij}, and total, g_{tot}, radial distribution functions for a binary mixture with $N = 20, x_1 = 1/2, \mu_1 = 1, \mu_2 = 1836.15, \sigma = 0.4$. In the panel for the unlike radial distribution function we also show the ground state probability distribution of the Hydrogen atom for comparison. The mixture is in a thermodynamic state with a reduced temperature $T = T'/\mathscr{T} = 0.1$ with T' measured in degrees Kelvin and a reduced number density $n = n'\mathscr{L}^3 = 0.08$ with n' measured in cm^{-3}. In the path integral we chose $M = 20$ and used either Bose-Einstein (case C in Table I) or Fermi-Dirac (case D in Table I) statistics among like particles. In the figures $r = r'/\mathscr{L}$ where r' is measured in centimeters.

In Fig. 16 of Ref. [5] they found, using the coupled electron-ions PIMC, some evidence for the H_2 molecule formation at $T = 1200\mathrm{K}/\mathscr{T} \approx 3.80017 \times 10^{-3}$ and $r_s = 1.44$ which means $n \approx 0.159902$. This is made manifest by the development of a pronounced first peak in the proton-proton RDF at these low temperatures. In Fig. 6 we present the RDF that we measured close to that thermodynamic state. Even if we use a number of particles, N, and a number of timeslices, M, much smaller than the ones used in Ref. [5], we see how our unlike RDFs develops a pronounced peak near one Bohr radius, at contact of two hard core ions, as expected by the formation of H_2 molecules. Moreover we also see the appearance of a second peak, much more damped, at two Bohr radii which can be interpreted as a trace of the formation of H_3 linear molecules. At this low temperature also the protons paths begin to show a certain extension so that they cannot be treated classically anymore. Nonetheless their superfluid fraction is still very close to zero and their exchanges we observe in the simulation are negligible. In these cases, contrary to the other cases treated, also the superfluid fraction of the electrons component is almost zero. This is due to the fact that at this low temperature the electrons do not have enough kinetic energy to escape the Coulomb attraction towards the protons. And each electron is captured by one proton in a H atom.

Note that instead of the additive mixture of Eq. (2.10) we could use a nonadditive one in the Widom-Rowlinson limit [7, 12] with

$$\mathbf{\Sigma} = \begin{pmatrix} 0 & \sigma/2 \\ \sigma/2 & 0 \end{pmatrix}. \tag{2.14}$$

We repeated for this new scenario the simulations of cases G and H. In Fig. 7 we show the partial and total RDF that we obtained. From the figure we see how there is a sensible difference between the Fermi-Dirac and the Bose-Einstein

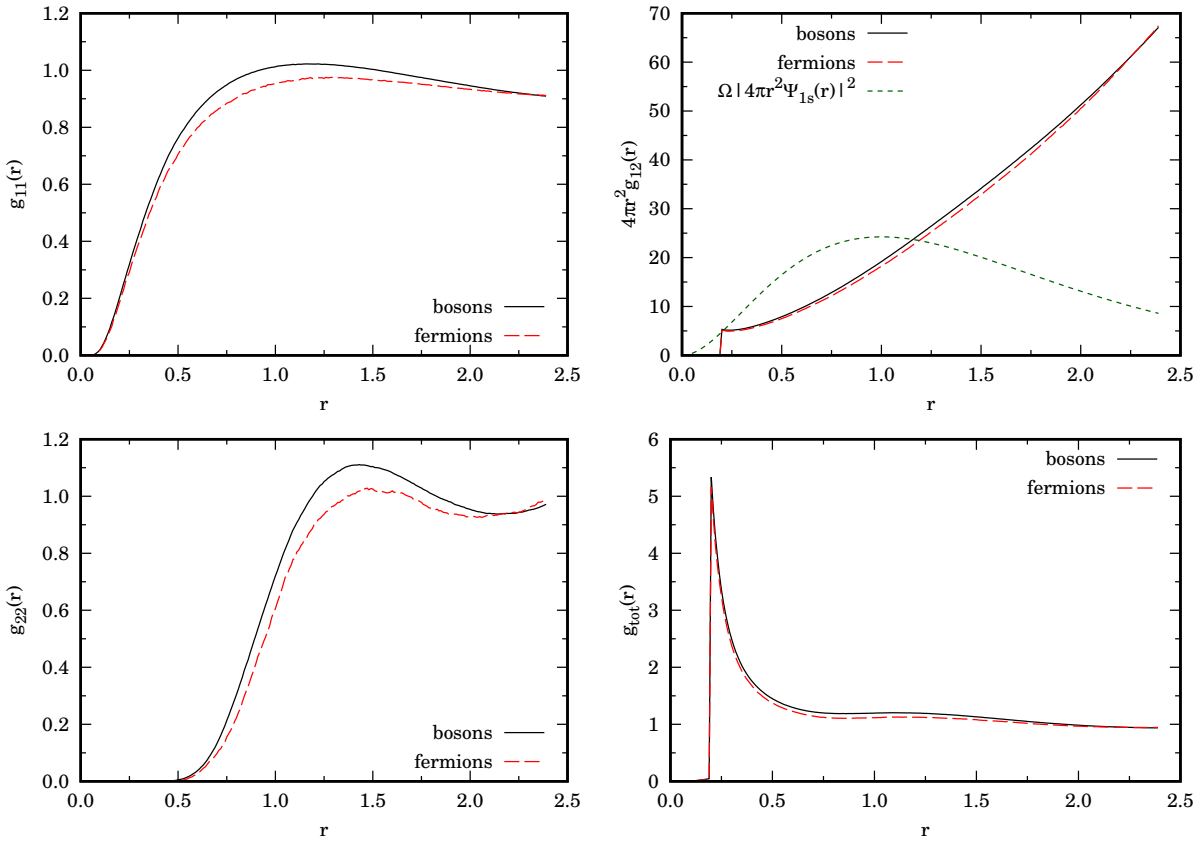

FIG. 5. The partial, g_{ij}, and total, g_{tot}, radial distribution functions for a binary mixture with $N = 20, x_1 = 1/2, \mu_1 = 1, \mu_2 = 1836.15, \sigma = 0.4$. In the panel for the unlike radial distribution function we also show the ground state probability distribution of the Hydrogen atom for comparison. The mixture is in a thermodynamic state with a reduced temperature $T = T'/\mathscr{T} = 0.1$ with T' measured in degrees Kelvin and a reduced number density $n = n'\mathscr{L}^3 = 0.18$ with n' measured in cm^{-3}. In the path integral we chose $M = 20$ and used either Bose-Einstein (case E in Table I) or Fermi-Dirac (case F in Table I) statistics among like particles. In the figures $r = r'/\mathscr{L}$ where r' is measured in centimeters.

statistics. For fermions the peaks of the partial RDF are shifted at smaller radii than for bosons. In particular the reduced radius of the H_2 molecule, the first peak in g_{22}, is ≈ 0.95 in the Bose-Einstein case and ≈ 0.85 in the Fermi-Dirac case. Note that even if we did not explicitly impose a hard core among the protons nonetheless the first peak in g_{22} approximately coincides with the additive case with $\sigma = 1$. Moreover the second peak disappears for the fermions case. On the other hand g_{11} presents a shoulder preceding its first peak in the bosons case that disappears in the fermions case. Once again the first peak in this nonadditive case approximately coincides with the previous additive case.

III. CONCLUSIONS

We simulated with the path integral Monte Carlo method a quantum binary mixture where the like particles obeys either to the Bose-Einstein, using an *exact* PIMC calculation, or to the Fermi-Dirac statistics, using an *approximate* RPIMC. We used as pair interaction among the particles the Coulomb $1/r$ interaction assuming total neutrality of the mixture (so to ensure thermodynamic stability) and considered the case with repulsion between like particles and attraction among unlike particles. This is a Two Component Plasma (TCP). We then specialized our TCP to the case of the electron-proton plasma with 1:1 ratio between the molar fractions of the two species. This allowed us to investigate the formation of H atoms predicted simply by the laws of quantum statistical physics and of Coulomb. To stabilize the plasma against collapse of the electrons onto the protons we needed to introduce a spherical hard core of diameter σ for the protons with the electrons left pointwise. We considered both the additive and nonadditive cases.

We then started at high enough temperature, T, to ensure a ionized plasma and gradually lowered it. We first

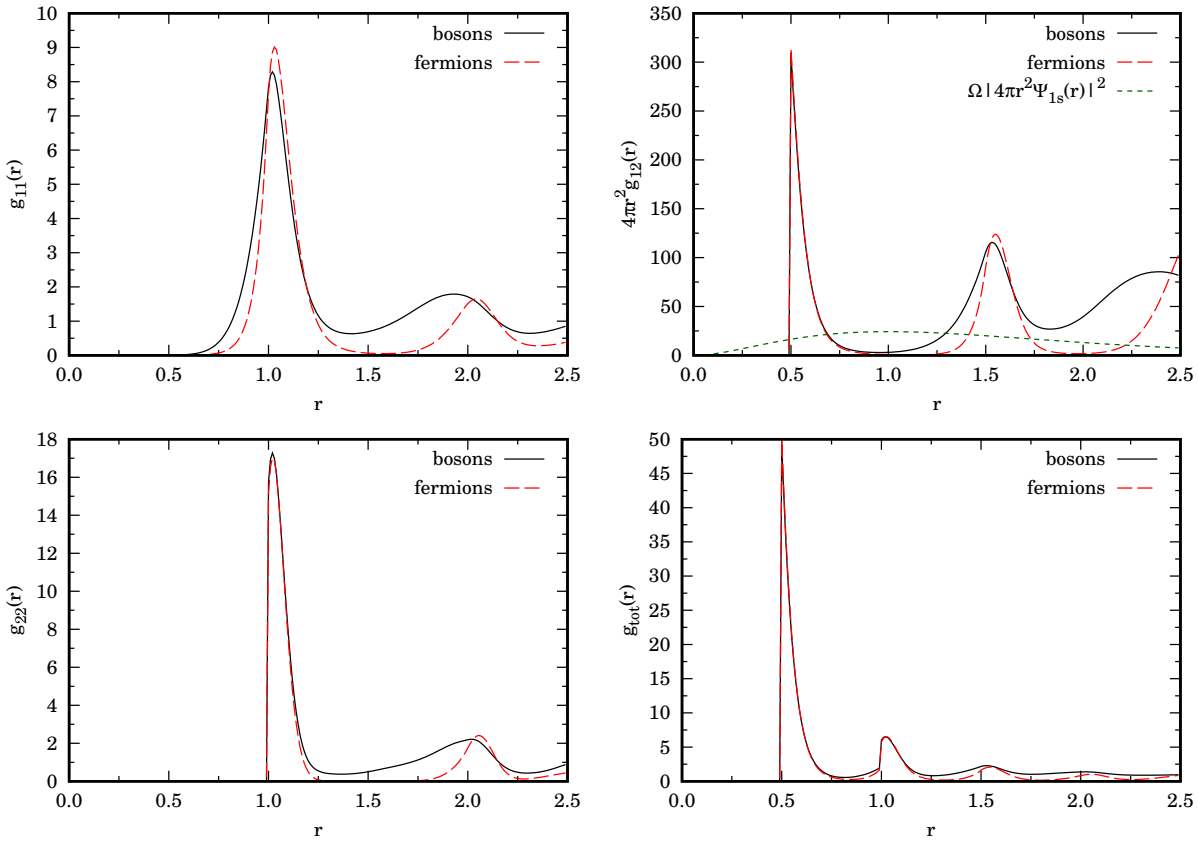

FIG. 6. The partial, g_{ij}, and total, g_{tot}, radial distribution functions for a binary mixture with $N = 20, x_1 = 1/2, \mu_1 = 1, \mu_2 = 1836.15, \sigma = 1$. In the panel for the unlike radial distribution function we also show the ground state probability distribution of the Hydrogen atom for comparison. The mixture is in a thermodynamic state with a reduced temperature $T = T'/\mathscr{T} = 0.005$ with T' measured in degrees Kelvin and a reduced number density $n = n'\mathscr{L}^3 = 0.16$ with n' measured in cm^{-3}. In the path integral we chose $M = 20$ and used either Bose-Einstein (case G in Table I) or Fermi-Dirac (case H in Table I) statistics among like particles. In the figures $r = r'/\mathscr{L}$ where r' is measured in centimeters.

observed the formation of H atoms resulting in a metallic Hydrogen phase by looking at the unlike RDF which develops a strong peak at contact between the pointwise electron and the hard core ion. We also saw that increasing the density makes the two components behave more like free gases.

Lowering the temperature even more we observed that a phase transition of the electron-proton plasma from a metallic phase with mostly delocalized electrons as in Figs. 4 and 5 to a molecular fluid phase as in Fig. 6. Looking at the total RDF g_{tot} of Fig. 6 we then see that the first peak is the result of the H atom formation whereas the second peak reflects the H_2 molecule formation.

The same result could have been obtained by keeping the temperature constant and lowering the ions hard core diameter σ. This unphysical freedom however is only apparent and required by the primitive approximation [8] which is unbounded from below for the electron-proton interaction and therefore breaks down the Trotter approximation [15] giving rise to the path integral expression for the density matrix. Instead of introducing hard cores, an alternative way out of this problem, is to truncate the unlike Coulomb potential artificially as

$$\phi_{ij}(r) = \begin{cases} \epsilon_{ij}/r & r > \Sigma_{ij} \\ \epsilon_{ij}/\Sigma_{ij} & \text{else} \end{cases} \qquad i \neq j, \tag{3.1}$$

choosing $\sigma = 2r_0$ from Eq. (2.5). Otherwise a route free of any artificial parameter is to use the pair Coulomb density matrix [8, 13] for the unlike component instead of the usual primitive approximation. It is interesting to stress that this is only possible in quantum statistical physics and in classical statistical physics the hard core between unlike species is an unavoidable feature necessary to grant stability of a neutral TCP.

Regarding the comparison between the simulations using Bose-Einstein or Fermi-Dirac statistics between like particles we noticed a sensible difference for the nonadditive mixture below the partial degeneracy temperatures. The

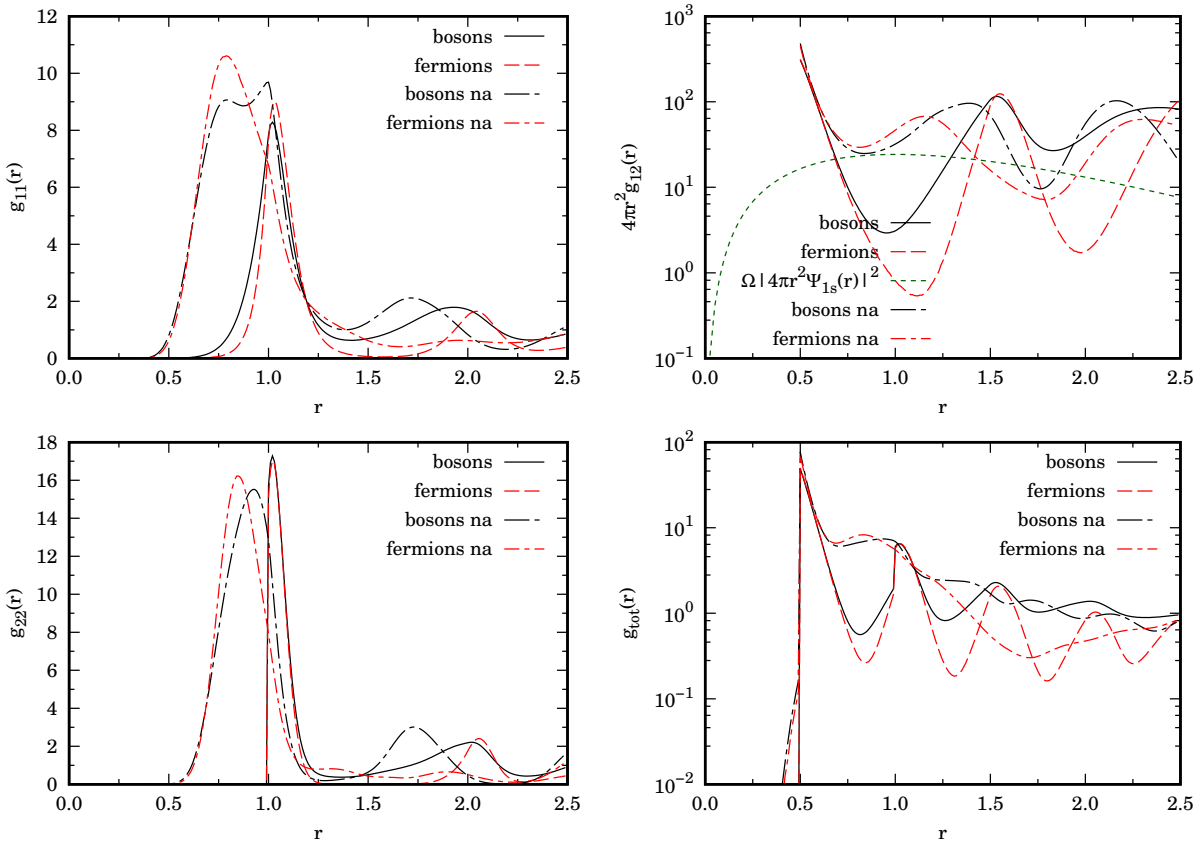

FIG. 7. The partial, g_{ij}, and total, g_{tot}, radial distribution functions for the nonadditive (na) binary mixture of Eq. (2.14) with $N = 20, x_1 = 1/2, \mu_1 = 1, \mu_2 = 1836.15, \sigma = 1$. In the panel for the unlike radial distribution function we also show the ground state probability distribution of the Hydrogen atom for comparison. The mixture is in a thermodynamic state with a reduced temperature $T = T'/\mathscr{T} = 0.005$ with T' measured in degrees Kelvin and a reduced number density $n = n'\mathscr{L}^3 = 0.16$ with n' measured in cm^{-3}. In the path integral we chose $M = 20$ and used either Bose-Einstein (case G in Table I) or Fermi-Dirac (case H in Table I) statistics among like particles. In the figures $r = r'/\mathscr{L}$ where r' is measured in centimeters. We also report the partial RDF of Fig. 6 for comparison. We use a logarithmic scale for the unlike and the total RDF.

difference still persists for the heavy protons component due to their interaction with the light electrons component. From Fig. 7 we see how for the nonadditive case in the Widom-Rowlinson limit, where the hard cores of the like particles is set to zero and the one of the unlike particles is set to $\sigma/2$, we find that the protons component develops a H_2 first peak at a radius slightly smaller than in the case of the additive mixture with a protons hard core equal to σ. Moreover the second peak almost disappears in the fermions case. This can be explained by the fact that the electrons cloud around each proton produce a "dressed" proton. These dressed protons like to form H_n molecules with $n = 2$, slightly smaller than the H_2 molecules formed in the additive mixture, and no other $n > 2$ molecules, unlike the additive mixture.

Looking ahead to the simulation of the real electron-proton plasma in nature we must take care of the following points: i. Use the pair Coulomb density matrix to eliminate the artificial hard core necessary to treat the primitive approximation; ii. Carefully asses the convergence towards the continuum limit. This requires to choose τ so that the standard deviations for the free particle diffusions of the two species be both much smaller than the size of the simulation box, i.e. $\sigma_i = \sqrt{\tau/\mu_i} \ll L$, $i = 1, 2$ [4] ; iii. Choose carefully the thermodynamic state of temperature and density to reproduce. Being it for a planet interior like the one for Jupiter [16] or for earthly laboratory conditions like the one of high pressures under diamond anvil cells [17].

[4] For example in the simulation of Fig. 6 and 7 we have $L = 5$ and $\sigma_e = 3.16228, \sigma_p = 0.0737982$. So this condition is not really satisfied.

Appendix A: Description of our PIMC and RPIMC algorithms

Our PIMC algorithm is made of two kinds of moves: a single slice move and a multislice move [8]. In the single slice move we perform a uniform displacement of a single particle coordinate at a given timeslice. We accept or reject the move according to the Metropolis algorithm [11, 18]. In the multislice move we create two Brownian bridges [11] between the initial positions taken from the paths of two particles α and γ at the same timeslice and the final positions taken from the same two paths at a subsequent timeslice but exchaged, γ and α, so to connect particle α at the initial timeslice to particle γ at the final timeslice with one bridge and particle γ at the initial timeslice with particle α at the final timeslice. Again we accept or reject the move according to Metropolis algorithm. If the move is accepted one creates an exchange of two particles. Since any permutation of N_i particles can be obtained by composing a finite number of like particles exchanges this is sufficient to simulate Bose-Einstein statistics in an exact numerical way. For Fermi-Dirac statistics one will face the "fermions sign problem" [9]. In order to overcome this it is necessary to use an approximate algorithm. We chose the RPIMC described in Ref. [10] enforcing a free particle (approximate) restriction during the simulation.

The listing of our FORTRAN code is given in the supplemental material.

AUTHOR DECLARATIONS

Conflicts of interest

None declared.

Data availability

The data that support the findings of this study are available from the corresponding author upon reasonable request.

Funding

None declared.

[1] A. Lenard, Exact Statistical Mechanics of a One Dimensional System with Coulomb Forces, J. Math. Phys. **2**, 682 (1961).
[2] S. F. Edwards and A. Lenard, Exact Statistical Mechanics of a One Dimensional System with Coulomb Forces. II. The Method of Functional Integration, J. Math. Phys. **3**, 778 (1961).
[3] D. M. Ceperley and B. J. Alder, The Calculation of the Properties of Metallic Hydrogen using Monte Carlo, Physica B **108**, 875 (1981).
[4] C. Pierleoni, B. Bernu, D. M. Ceperley, and W. R. Magro, Equation of State of the hydrogen plasma by path integral Monte Carlo simulation, Phys. Rev. Lett. **73**, 2145 (1994).
[5] M. Bonitz et al., Towards first principles-based simulations of dense hydrogen, Physics of Plasma **31**, 110501 (2024).
[6] C. Pierleoni, D. M. Ceperley, and M. Holzmann, Coupled Electron Ion Monte Carlo Calculations of Dense Metallic Hydrogen, Phys. Rev. Lett. **93**, 146402 (2004).
[7] R. Fantoni and G. Pastore, Monte Carlo simulation of the nonadditive restricted primitive model of ionic fluids: Phase diagram and clustering, Phys. Rev. E **87**, 052303 (2013).
[8] D. M. Ceperley, Path integrals in the theory of condensed Helium, Rev. Mod. Phys. **67**, 279 (1995).
[9] D. M. Ceperley, Fermion Nodes, J. Stat. Phys. **63**, 1237 (1991).
[10] D. M. Ceperley, Path integral Monte Carlo methods for fermions, in *Monte Carlo and Molecular Dynamics of Condensed Matter Systems*, edited by K. Binder and G. Ciccotti (Editrice Compositori, Bologna, Italy, 1996).
[11] M. H. Kalos and P. A. Whitlock, *Monte Carlo Methods* (John Wiley & Sons Inc., New York, 1986).
[12] R. Fantoni and G. Pastore, Direct correlation functions of the Widom-Rowlinson model, Physica A **332**, 349 (2004).
[13] E. L. Pollock, Properties and computation of the Coulomb pair density matrix, Comput. Phys. Commun. **52**, 49 (1988).
[14] V. Natoli and D. M. Ceperley, An Optimized Method for Treating Long-Range Potentials, Comput. Phys. **117**, 171 (1995).
[15] H. F. Trotter, On the Product of Semi-Groups of Operators, Proc. Am. Math. Soc. **10**, 545 (1959).
[16] D. Saumon and T. Guillot, Shock compression of deuterium and the interiors of Jupiter and Saturn, Astrophys. J. **609**, 1170 (2004).

[17] R. J. Hemley and H. K. Mao, Phase transition in solid molecular hydrogen at ultrahigh pressures, Phys. Rev. Lett. **61**, 857 (1988).
[18] N. Metropolis, A. W. Rosenbluth, M. N. Rosenbluth, A. M. Teller, and E. Teller, Equation of state calculations by fast computing machines, J. Chem. Phys. **1087**, 21 (1953).